

RESEARCH ARTICLE

Tunable alginate hydrogels as injectable drug delivery vehicles for optic neuropathy

Courtney J. Maxwell¹ | Andrew M. Soltisz¹ | Wade W. Rich¹ | Andrew Choi¹ |
Matthew A. Reilly^{1,2}  | Katelyn E. Swindle-Reilly^{1,2,3} 

¹Department of Biomedical Engineering, The Ohio State University, Columbus, Ohio, USA

²William G. Lowrie Department of Chemical and Biomolecular Engineering, The Ohio State University, Columbus, Ohio, USA

³Department of Ophthalmology and Visual Sciences, The Ohio State University, Columbus, Ohio, USA

Correspondence

Katelyn E. Swindle-Reilly, Department of Biomedical Engineering, The Ohio State University, 3010 Fontana Labs, 140 W 19th Ave, Columbus, OH 43210, USA.
Email: reilly.198@osu.edu

Funding information

U.S. Department of Defense, Grant/Award Number: W81XWH-15-1-0074

Abstract

Many disease pathologies, particularly in the eye, are induced by oxidative stress. In particular, injury to the optic nerve (ON), or optic neuropathy, is one of the most common causes of vision loss. Traumatic optic neuropathy (TON) occurs when the ON is damaged following blunt or penetrating trauma to either the head or eye. Currently, there is no effective treatment for TON, only management options, namely the systematic delivery of corticosteroids and surgical decompression of the optic nerve. Unfortunately, neither option alleviates the generation of reactive oxygen species (ROS) which are responsible for downstream damage to the ON. Additionally, the systemic delivery of corticosteroids can cause fatal off-target effects in cases with brain involvement. In this study, we developed a tunable injectable hydrogel delivery system for local methylene blue (MB) delivery using an internal method of crosslinking. MB was chosen due to its ROS scavenging ability and neuroprotective properties. Our MB-loaded polymeric scaffold demonstrated prolonged release of MB as well as in situ gel formation. Additionally, following rheological characterization, these alginate hydrogels demonstrated minimal cytotoxicity to human retinal pigment epithelial cells in vitro and exhibited injection feasibility through small-gauge needles. Our chosen MB concentrations displayed a high degree of ROS scavenging following release from the alginate hydrogels, suggesting this approach may be successful in reducing ROS levels following ON injury, or could be applied to other ocular injuries.

KEYWORDS

alginate, controlled release, hydrogel, methylene blue, ocular drug delivery, optic neuropathy, reactive oxygen species

1 | INTRODUCTION

The optic nerve (ON) is a component of the central nervous system responsible for transmitting visual information from the eye to the brain. Optic neuropathy results in visual dysfunction due to optic

nerve pathology (e.g., glaucoma) and can be caused by several mechanisms, including ischemia, malnutrition, chemical toxicity, tumor or immunological insult, or trauma. Traumatic optic neuropathy (TON) is an ocular injury in which the force or motion of the globe or orbital tissues is transferred from the eye or skull to the optic nerve. It can be

This is an open access article under the terms of the [Creative Commons Attribution-NonCommercial](https://creativecommons.org/licenses/by-nc/4.0/) License, which permits use, distribution and reproduction in any medium, provided the original work is properly cited and is not used for commercial purposes.

© 2022 The Authors. *Journal of Biomedical Materials Research Part A* published by Wiley Periodicals LLC.

characterized by transient or permanent vision impairment, associated vascular damage and edema, and subsequent ON atrophy.¹ In civilians, 0.4% of trauma patients incur TON; this increases to 5% in cases involving closed-head injuries.^{2,3} Among soldiers, its incidence is higher, with ocular trauma representing up to 13% of recent battlefield injuries.⁴ The current management options for the treatment of TON are inadequate and include the systemic delivery of corticosteroids and surgical decompression of the nerve. Both treatments are ineffective at improving visual recovery, have side effects such as optic atrophy, complications following surgical decompression,⁵ and do not address secondary injury mechanisms such as the unattenuated generation of reactive oxygen species (ROS).⁶ Moreover, systemic delivery of suitable agents is contraindicated owing to the presence of additional sources of trauma as they can cause additional injury and even cellular death.¹ The ability to deliver therapeutics locally to the eye or ON is therefore essential for improving outcomes for TON patients.

Prolonged exposure to high ROS levels is known to disrupt normal physiology in many systems, particularly in the eye, inducing damage to cellular organelles and processes.⁵ In the ON, high levels of ROS can cause a multitude of cellular dysregulations, namely the migration of inflammatory cells to the site of injury. These secondary injuries contribute to the formation of glial scarring,⁶ preventing tissue recovery by inhibiting signal transduction following the primary injury and contributing to permanent vision loss. Inhibition of oxidative stress using ROS scavengers is therefore an appealing therapeutic modality for mitigating secondary neurodegeneration.

Methylene blue (MB) is a potent ROS scavenger and neuroprotective agent capable of crossing the blood–brain barrier with a demonstrated inhibitory effect on glial cell migration *in vivo*.^{7–11} These qualities, along with recent discoveries of recovery following traumatic brain injury (TBI) and stroke in rats,^{12,13} makes MB a promising therapeutic candidate for TON treatment. Due to its low molecular weight and high-water solubility, direct local injection of MB to the ON would

be inadequate, leading to rapid diffusion of MB away from the site of injury. By surrounding the injured nerve with a MB-loaded degradable scaffold, we hypothesize that drug elution would be better facilitated, allowing for a more sustained therapeutic release. The novelty of this study is the use of a tunable injectable hydrogel loaded with a neuroprotective and ROS scavenging agent. A recent study demonstrated delivery of erythropoietin through microparticles to scavenge ROS for treatment of TON, demonstrating further potential of this approach.¹⁴

Alginate-based hydrogels were selected as the drug delivery vehicle in our study due to their biocompatible nature and extensive usage in tissue engineering and drug delivery applications.^{15,16} Typically, aqueous alginate is externally crosslinked by the addition of dissolved Ca^{2+} ions, forming a hydrated scaffold. This method was initially investigated for our TON treatment, but it induced rapid gelation, limiting its injection feasibility through a small gauge needle. Draget et al.,¹⁷ introduced an internal method of alginate crosslinking (Figure 1), in which insoluble calcium carbonate (CaCO_3) particles are evenly distributed throughout the alginate solution before the addition of a slow hydrolyzing proton donor, in our case, D-glucono-lactone (GDL). Alginate is a polysaccharide composed of two residues, (1–4)-linked β -D-mannuronate (M), and α -L-guluronate (G). The internal method of crosslinking slows the process of gelation to a rate that accommodates mixing of all components, subsequent injection through a small gauge needle, and *in situ* hydrogel formation. By modulating the concentrations of the hydrogel's constituents in this study, we developed a hydrated polymeric scaffold with tunable mechanical properties and gelation times. Previous studies have evaluated alginate gels crosslinked with CaCO_3 as an injectable vehicle for osteoblast delivery in tissue engineering applications^{18–20}; however, an extensive evaluation of its drug delivery capabilities has yet to be studied, which we addressed in this study. Given the need for a TON treatment that addresses the current limitations, internally crosslinked MB-loaded injectable alginate hydrogels could potentially lower levels of ROS and effectively improve visual recovery following injury,

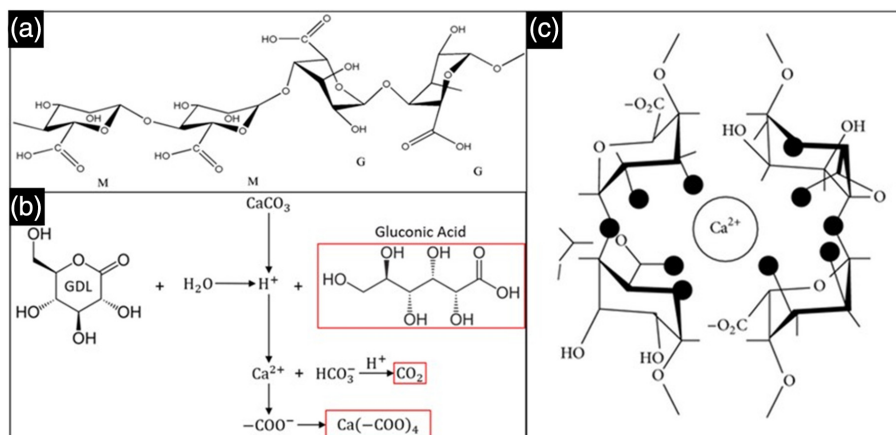


FIGURE 1 Diagram of crosslinking reaction and final hydrogel structure. (a) Alginate is a polysaccharide copolymer composed of two residues, (1–4)-linked β -D mannuronate (M), and α -L-guluronate (G).³⁸ The patterning and ratio of these residues can significantly impact the material properties of alginate gels. (b) Schematic of the crosslinking reaction between the proton donor D-glucono-lactone (GDL), the calcium ion source CaCO_3 and the alginate polymer. The reaction generates three products—gluconic acid, carbon dioxide, and the calcium ion-alginate complex. (c) Once Ca^{2+} is freed by GDL, the free ion interacts with alginate's carboxyl group to form ionic crosslinks between polymers.³⁹

representing a potentially significant advancement over the current treatment methodology.

With the above considerations, the purpose of this study was to use design of experiments to synthesize tunable alginate hydrogels loaded with MB through internal crosslinking and in situ gelation. Modulation of hydrogel properties using statistical methods enables prediction of delivery system properties,²¹ providing an opportunity to tailor the properties for specific drug delivery applications, particularly in the eye. We hypothesized that MB stimulated by oxidative stress could achieve ROS scavenging and effectively halt the generation of deleterious reactive species, representing a potential new treatment option for optic neuropathies and traumatic ocular injuries.

2 | MATERIALS AND METHODS

2.1 | Materials

Sodium alginate (Protanal PH 1033, M/G ratio 55–65/35–45, 300–800 mPa-s viscosity at 0.5%) was provided by FMC Biopolymer (Philadelphia, Pennsylvania). Methylene blue (MB) and Dulbecco's

phosphate-buffered saline (DPBS) were purchased from Sigma-Aldrich (Saint Louis, Missouri). Calcium carbonate (CaCO₃) was purchased from ChemProducts (Tualatin, Oregon). D-(+)-glucono-1,5-lactone (GDL) was purchased from Alfa Aesar (Haverhill, Massachusetts). Colorimetric 3-(4,5-dimethylthiazol-2-yl)-5-(3-carboxymethoxyphenyl)-2-(4-sulfonyl)-2H-tetrazolium (MTS) assay and 2,7-dichlorodihydrofluorescein diacetate (DCFH-DA) assay were purchased from Fisher Scientific Inc. (Hampton, New Hampshire). Human retinal pigment endothelial cells (ARPE-19, ATCC CRL-2302) were purchased from American Type Culture Collection (ATCC) (Manassas, Virginia). Dulbecco's Modified Eagle's/Nutrient Mixture F-12 Ham's Medium (DMEM/F-12), phenol-free DMEM, fetal bovine serum (FBS), penicillin-streptomycin (PS), trypsin, dimethyl sulfoxide (DMSO) and hydrogen peroxide (H₂O₂) were all purchased from Thermo Fisher Scientific (Waltham, Massachusetts).

2.2 | Hydrogel synthesis

Alginate hydrogels were prepared based on methods reported in literature with modifications.¹⁹ Twenty one total hydrogel formulations were prepared and evaluated using design of experiments to modify

TABLE 1 Composition of hydrogel formulations prepared and evaluated

Formulation ID	Formulation name	Ca ²⁺ :Alginate monomer (mol:mol)	GDL:CaCO ₃ (mol:mol)	[CaCO ₃] (mg/ml)	[GDL] (mg/ml)
1	C/G 1.6/7.1	0.469	2.493	1.6	7.1
2	C/G 2.5/7/1	0.733	1.596	2.5	7.1
3	C/G 3.4/7.1	0.997	1.173	3.4	7.1
4	C/G 1.6/9.4	0.469	3.301	1.6	9.4
5	C/G 2.5/9.4	0.733	2.113	2.5	9.4
6	C/G 3.4/9.4	0.997	1.553	3.4	9.4
7	C/G 1.6/11.7	0.469	4.109	1.6	11.7
8	C/G 2.5/11.7	0.733	2.630	2.5	11.7
9	C/G 3.4/11.7	0.997	1.933	3.4	11.7
10-L	C/G 0.4/0.4	0.500	0.125	0.4	0.4
11	C/G 0.9/0.8	0.500	0.250	0.9	0.8
12	C/G 1.7/1.5	0.500	0.500	1.7	1.5
13	C/G 3.4/3.0	0.500	1.000	3.4	3.0
14	C/G 0.4/0.8	1.000	0.125	0.4	0.8
15	C/G 0.9/1.5	1.000	0.250	0.9	1.5
16-M	C/G 1.7/3.0	1.000	0.500	1.7	3.0
17	C/G 3.4/6.1	1.000	1.000	3.4	6.1
18	C/G 0.4/1.1	1.500	0.125	0.4	1.1
19	C/G 0.9/2.3	1.500	0.250	0.9	2.3
20	C/G 1.7/4.6	1.500	0.500	1.7	4.6
21-H	C/G 3.4/9.1	1.500	1.000	3.4	9.1

Note: The alginate hydrogels were designed based on their ability to form solid homogenous hydrogels. Formulations consisted of 180 mg sodium alginate with varying molar concentrations of CaCO₃ and GDL. The final GDL and CaCO₃ concentrations were modulated based on preliminary hydrogels (1–9). Molar concentrations of GDL:CaCO₃ ratios ranged from 0.125 to 1.00. Aqueous 1 mg/ml MB was also added to each formulation, except in ROS studies in which MB ranged from 0.05 to 2.0 mg/ml to assess the influence of MB concentration on ROS scavenging ability. In select studies, formulations 10, 16, and 21 were further evaluated and labeled as L, M, or H, for low, medium, and high concentrations. The second column denotes a naming scheme with ratio of [CaCO₃]/[GDL].

alginate, CaCO_3 and GDL concentrations. The first nine formulations were selected based on their consistency in forming solid homogeneous hydrogels (Table 1). These nine gels served as the models for pH testing in preliminary experiments (see Section 2.4).

Briefly, sodium alginate (0.63%–1.85% final w/v in gel) was dissolved in deionized (DI) H_2O by vortexing for 30 s and heating in 37°C water for 24 h. Aqueous 1 mg/ml MB was added to a final concentration of 0.05 mg/ml, followed by the addition of CaCO_3 and vortexed. As gelation is initiated rapidly following addition of GDL, the solution was quickly transferred to a mold or onto the rheometer stage following subsequent mixing of all components.

To prepare the remaining hydrogel formulations (10–21), GDL: CaCO_3 molar ratio concentrations were based off of the original nine formulations that exhibited a neutral pH of 7.0 ± 1.0 (Table 1, Figure 2), which would be more suitable for biomedical application. These GDL: CaCO_3 ratios ranged from 0.125 to 1.00. The Ca^{2+} :alginate monomer molar ratios were also evaluated as a design factor and varied from 0.5 to 1.5. The ratios were selected to assess the influence of alginate and crosslinker concentrations on drug release, gelation time, and viscoelastic properties. Hydrogel formulations were selected as representative low (L), medium (M) and high (H) concentration hydrogels due to GDL: CaCO_3 molar ratios of 0.125, 0.500, and 1.00 (formulations

10, 16, 21, or L-10, M-16, and 21-H, respectively). These three formulations were further analyzed in cytotoxicity and ROS experiments (see Sections 2.8 and 2.9).

2.3 | Cell culture

A human retinal pigment epithelial cell line (ARPE-19, ATCC[®] CRL-2302[™]) was selected for in vitro studies due to its availability and use as a standard cell line for ocular toxicity and ROS studies. Cells were cultured in DMEM/F-12 supplemented with 10% FBS and 1% PS at 37°C and 5% CO_2 and were used for in vitro analysis at 80% confluency.

2.4 | Hydrogel pH

The pH values of alginate hydrogel formulations 1–9 were evaluated using a calibrated pH probe (Mettler Toledo, InLab Expert Pro-ISM, Columbus, Ohio) for 72 h to evaluate pH evolution over time. These tests were then used to inform the final compositions of hydrogel formulations 10–21. The final pH after 72 h was reported as the equilibrium pH (pH_E).

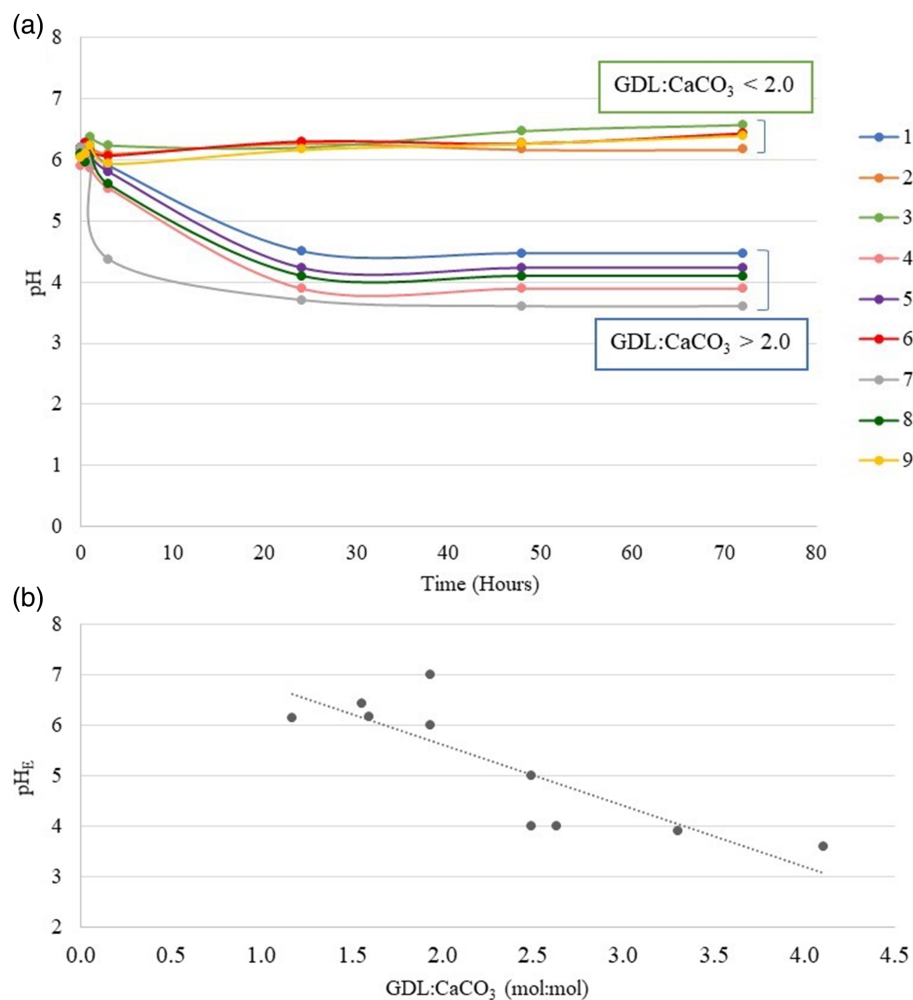


FIGURE 2 Characterization of pH of hydrogel formulations 1–9. (a) Evolution of hydrogel pH over 72 h. Formulations exhibit clear groupings of pH values ($n = 3$). (b) Plot of hydrogel equilibrium pH (pH_E) reached after 72 h of gelation. There is a linear and inverse relationship between GDL: CaCO_3 and pH_E with an R^2 of 0.8 ($p < .0001$) ($n = 3$).

2.5 | Gelation kinetics and mechanical properties

Oscillatory shear rheology was used to characterize the gelation kinetics, strain amplitude response, and frequency response of alginate hydrogel formulations 10–21.²² The rheometer used was a Malvern Panalytical Kinexus Ultra+ (Malvern, United Kingdom) with a 20 mm titanium parallel plate upper geometry (PU20 SW1511 TI) and aluminum lower geometry (PLC61 S3722 AL). For all rheological tests, the gap height between the lower and upper geometries, the temperature and sample size were kept constant at 1 mm, 37°C and 375 μ l, respectively.

To measure the gelation kinetics of alginate hydrogels, the alginate solution was dispensed as a liquid directly onto the lower geometry of the rheometer immediately following the addition and mixing of GDL. A constant frequency and strain amplitude of 1 Hz and 1% respectively (within linear viscoelastic region), were applied to the sample with its resulting shear stress measured every 5 s for 2 h. The gelation time was defined as the time which gelation had terminated and was determined from the constant frequency and strain test as the first timepoint where complex shear modulus (G^*) did not increase by more than 1% of the average of the 10 previously collected measurements.²² A frequency sweep test immediately followed the gelation test, evaluating the frequency response of the hydrogel. Here, a constant strain amplitude of 1% was applied to the sample while frequency increased from 1 to 100 Hz. The stiffness of the hydrogels is reported as the value of G^* at 1 Hz from frequency sweep tests.

Representative low, medium, and high concentration CaCO_3 and GDL hydrogels (formulations 10-L, 16-M, and 21-H, or C/G 0.4/0.4, 1.7/3.0, 3.4/9.1, respectively) were additionally subjected to an amplitude sweep test to evaluate strain amplitude response. A constant frequency of 1 Hz was applied to the sample while the strain amplitude increased from 0.1% to 100%, and resulting stress was measured. All rheological studies were repeated ($n = 3$) for formulations 10-L, 16-M, and 21-H both with and without the addition of 1 mg/ml MB.

2.6 | Hydrogel swelling and MB release

One milliliter samples of hydrogel formulations 10–21 were cast in pre-weighed 15 ml conical tubes and weighed. Hydrogels were then immersed in 1 ml DPBS at 37°C and at regular intervals (0, 1, 3, 7, and 14 days), DPBS was removed and the mass of the hydrogels was recorded. Results were calculated according to the following equation:

$$Q = \frac{M_S - M_D}{M_D} \times 100\%$$

where Q is the swelling ratio, M_S is the mass of the formed hydrogel following incubation in DPBS at 37°C and excess water removal and M_D is the mass of the 1 ml alginate solution placed in the tube.²³ The resulting hydrogels were cylindrical with 17 mm diameter and approximately 15 mm height. Formulations 1–9 were not included as

preliminary testing revealed GDL: CaCO_3 ratios of less than 2.0 yielded neutral pH values and, more specifically, GDL: CaCO_3 ratios of 0.25–1.0 had predetermined crosslinking maximums between Ca^{2+} ions and alginate. As such, the concentrations of GDL and CaCO_3 for the selected hydrogels ranged from 0.80 to 9.10 mg/ml and 0.40 to 3.40 mg/ml, respectively. All swelling studies were repeated ($n = 5$) for formulations 10-L, 16-M, and 21-H both with and without the addition of 1 mg/ml MB.

The release kinetics of MB were evaluated using the same formulations (10–21) evaluated for swelling, using published techniques for in vitro drug delivery evaluation for the ON.¹⁴ One milliliter hydrogels (10–21) loaded with 1 mg/ml MB were created. Following immersion in DPBS and incubation at 37°C, 1 ml DPBS was removed at the given intervals (0, 1, 3, 7, and 14 days). One hundred microliter samples of the DPBS were placed in a 96 well-plate and absorbance measured. The concentration of MB remaining in hydrogels following DPBS incubation was then determined using a standard concentration-absorbance curve measured at 630 nm using a plate reader (BioTekElx808, Winooski, Vermont). The standard curve was prepared with seven concentrations of MB from 0.625 to 40.0 μ g/ml plus a blank (0 μ g/ml). DPBS was used as it is the eluent that has been used for other in vitro ON release studies.¹⁴

2.7 | Hydrogel degradation

One milliliter hydrogel solutions based on formulations 10–21 were cast in pre-weighed 15 ml conical tubes and weighed. After incubation at 37°C for 72 h, excess water was removed from the tubes and hydrogels were weighed again to determine weight following incubation. Hydrogels of the same dimensions used in 2.6 were immersed in 10 ml 1X DPBS with MgCl_2 and CaCl_2 at 37°C for 0, 1, 3, 7, or 14 days. At each timepoint, the DPBS was removed, the hydrogels were frozen at -80°C for 24 h and lyophilized for 24 h. Hydrogel degradation was reported as the percentage change in the mass of dry components used to create the hydrogel to the dried hydrogel mass after lyophilization (Labconco, Kansas City, Missouri). All degradation studies were repeated ($n = 5$) for formulations 10-L, 16-M, and 21-H both with and without the addition of 1 mg/ml MB.

2.8 | Hydrogel cytotoxicity

The biocompatibility of representative low, medium and high GDL: CaCO_3 concentration hydrogels, ratios of 0.125, 0.500, and 1.00 (formulations 10-L, 16-M, 21-H, respectively), were evaluated using an MTS assay using methods adapted from Niu et al.²⁴ ARPE-19 cells were first seeded at 5×10^3 cells per well in 96-well clear bottom tissue culture (TC) plates and incubated for 24 h in 200 μ l base media (DMEM/F-12, 10% FBS, 1% PS). One milliliter hydrogels were formed in 15 ml conical tubes and allowed to completely gel for 72 h before 60 min UV light exposure to sterilize the gels prior to testing.²⁵ The hydrogels were then immersed in 1 ml base media for 24 h prior to

media collection. Cells were incubated in 200 μ l samples for 48 h prior to performing the MTS assay. A positive control of base media (DMEM/F-12, 10% FBS, 1% PS), negative control of 1:9 dimethyl sulfoxide (DMSO): growth media²⁶ and blank of phenol-free DMEM were used to validate the assay. After incubation, the hydrogel-soaked media was removed and each well washed three times with 200 μ l DPBS. Next, 180 μ l of phenol-free growth media and 20 μ l MTS reagent were added to each well and incubated for 4 h. Optical density (OD) of the MTS-treated media was measured at 490 nm using a BioTek Elx808 plate reader. All samples and controls were run in triplicate.

2.9 | ROS scavenging

A DCFH-DA assay was used to evaluate the ability of MB to scavenge ROS in cell culture based on the methods of Voloboueva et al.²⁷ ARPE-19 cells were seeded on 96 well plates at a density of 2×10^4 cells per well in DMEM/F-12 media supplemented with 10% FBS and 1% PS and incubated for 24 h. MB at concentrations of 0 mg/ml (positive control), 0.05, 0.25, 0.50, 1.0, and 2.0 mg/ml; a positive control of H₂O₂; and a negative control of DPBS were added to the wells and incubated for 24 h. Following incubation, the media was removed and 100 μ l of DCFH-DA solution was added to each well and incubated for 1–2 h. The cells were washed with DPBS once and the excitation and emission wavelengths, 485 nm and 535 nm, respectively, were measured using a microplate reader.

To further confirm the ROS scavenging ability of MB, 1 ml representative hydrogels (formulations 10-L, 16-M, 21-H) were formed in 15 ml conical tubes and allowed to gel for 72 h. Following gelation, the hydrogels were sterilized by exposure to UV light for 1 h. The hydrogels were then immersed in 1 ml base media for 24 h before media collection. ARPE-19 cells were seeded on a 96 well-plate with 2×10^4 cells per well in base growth media and allowed to grow for 24 h. The culture media was removed and the hydrogel-soaked medium was added to the wells. Hydrogen peroxide (10 μ l, 600 μ M final concentration) was added to test wells while DPBS was added to the other wells as a negative control. Hydrogel formulation 16-M (medium concentration C/G 1.7/3.0) without MB was included as an additional negative control. Cells were incubated for 24 h. Following incubation, the media was removed and 100 μ l of DCFH-DA solution was added to each well and incubated for 1–2 h. The cells were thoroughly washed with PBS, and the excitation and emission wavelengths were measured at 485 and 535 nm, respectively. All samples were run in triplicate, and tests were repeated at least three times.

2.10 | Injection feasibility

Four different hypodermic needle gauges (22, 25, 27, and 30-gauge) were used for the assessment of hydrogel injection feasibility. The hydrogels were loaded as both a liquid precursor and preformed gel into a 1 ml syringe connected to the needles. The needles chosen for

this study have similar diameters to others available for retrobulbar and intravitreal injections, which are performed clinically.^{28,29}

2.11 | Statistical analysis

Statistical analysis was performed using Microsoft Office Excel and R-Studio. Differences between two groups were compared using two-tailed Student's *t*-tests. Differences between more than two groups were tested using one-way analysis of variance (ANOVA) with post-hoc Bonferroni corrections or two-way ANOVA with post-hoc Tukey–Kramer pairwise comparisons. Statistical significance was defined as $p < 0.05$. All results are reported as the average \pm standard deviation (SD) with at least $n = 3$ replicates.

3 | RESULTS

3.1 | Hydrogel pH

The pH of hydrogel formulations 1–9 was recorded for 72 h (Figure 2A), with all formulations originating at pH \sim 6. Grouping among the hydrogels based on GDL:CaCO₃ molar ratios was initially observed around 10 h and continued through to the end of the study. Formulations 2, 3, 6, and 9 (C/G 2.5/7.1, 3.4/7.1, 3.4/9.4, 3.4/11.7) had ratios of 1.60, 1.17, 1.55, and 1.93, respectively. Their average final pH value (at 72 h) was 6.39 ± 0.17 . The remaining formulations, 1, 4, 5, 7, and 8 (C/G 1.6/7.1, 1.6/9.4, 2.5/9.4, 1.6/11.7, 2.5/11.7), had GDL:CaCO₃ ratios >2.0 ; 2.49, 3.30, 2.11, 4.11, and 2.63, respectively. Their average final pH value was much lower, 4.06 ± 0.33 . Additionally, a higher variability among the pH values of the more acidic hydrogels (1, 4, 5, 7, 8) was observed; however, the variability may be explained by the larger range of GDL:CaCO₃ ratios.

ANOVA was performed to analyze differences between the hydrogel formulations and their resulting pH values. It was determined that there were significant differences between the hydrogel formulations ($p = 6.6 \times 10^{-6}$) and their pH values ($p = 2.5 \times 10^{-5}$). A post-hoc Tukey test revealed further grouping among the hydrogels with significant differences between the ratios less than 2.0 and greater than 2.0. Formulations with ratios from 1.173 to 2.113 (formulations 2, 3, 6, 9) and ratios from 2.493 to 3.301 (formulations 1, 4, 5, 7, 8) were statistically different the other group ($p < 0.001$) but not within their groups ($p = 0.151$). A Student's two-sample *t*-test was performed analyzing the pH differences between formulations of GDL:CaCO₃ ratios less than and greater than 2.0 at various timepoints from the start of the study. It was determined that there was no statistical difference between the two groups at 0, 0.5, 1 and 3 h (p values 0.737, 0.476, 0.109, 0.112, respectively); however, there was a significant difference between the pH values of the two groups at 24, 48 and 72 h (p values 1.9×10^{-5} , 3.6×10^{-5} , and 2.5×10^{-5} , respectively). Greater molar concentrations of GDL and CaCO₃ caused significantly lower pH values as evidenced in Figure 2A.

TABLE 2 Quantification of the complex shear modulus and gelation times of hydrogels 10–21

Formulation ID	Formulation name	Gelation time (s)	G^* at 1 Hz (Pa)
10-L	C/G 0.4/0.4	2800 ± 40	36 ± 16
11	C/G 0.9/0.8	2035 ± 120	60 ± 21
12	C/G 1.7/1.5	1230 ± 85	125 ± 48
13	C/G 3.4/3.0	2000 ± 97	78 ± 15
14	C/G 0.4/0.8	2310 ± 20	60 ± 26
15	C/G 0.9/1.5	1540 ± 110	113 ± 53
16-M	C/G 1.7/3.0	1285 ± 250	247 ± 150
17	C/G 3.4/6.1	720 ± 60	560 ± 34
18	C/G 0.4/1.1	2190 ± 42	70 ± 34
19	C/G 0.9/2.3	1400 ± 80	190 ± 90
20	C/G 1.7/4.6	1070 ± 70	310 ± 140
21-H	C/G 3.4/9.1	675 ± 200	225 ± 110

Note: All hydrogels had a G^* of at least 35 Pa at 1 Hz and took at least 1 h to reach equilibrium stiffness ($n = 3$).

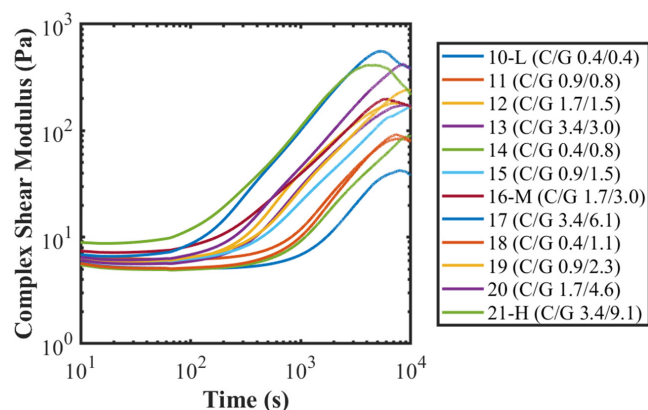


FIGURE 3 Gelation characterization of hydrogel formulations. Time sweep results of hydrogel formulations 10–21. Gelation times ranged from 707 ± 59 to 2803 ± 40 s ($n = 3$)

GDL:CaCO₃ molar ratios were plotted against pH_E over 72 h (Figure 2B). As determined previously, the molar concentration of GDL and CaCO₃ influenced formulation pH with greater molar concentrations of GDL and CaCO₃ contributing to a lower pH. As such, formulations close to neutral pH were evaluated in subsequent studies. Low, medium, and high concentration ratios were additionally selected based on this neutral pH. Ratios of 0.125, 0.5, and 1.0 were chosen as our low, medium, and high concentration hydrogels (10-L, 16-M, 21-H).

3.2 | Rheological characterization

Alginate hydrogel formulations 10–21 were prepared by varying CaCO₃ and GDL molar concentrations as shown in Table 1. Time sweep rheological analysis (Table 2, Figure 3) found that the different concentrations of the hydrogel components had an observable influence on complex shear modulus (G^*). As the concentrations of both

CaCO₃ and GDL increased, the complex shear modulus also increased. A two-way ANOVA with Tukey pairwise comparison revealed that complex shear moduli for formulations 12, 13, 15, 16, 17, 19, 20, and 21 were statistically different from each other ($p < 0.001$). These differences corresponded to hydrogels with increasing GDL content. As GDL releases H⁺ ions, the calcium ions in CaCO₃ are free to crosslink alginate. Although both GDL and CaCO₃ are required for crosslinking alginate via this mechanism, an increasing availability of calcium ions through GDL concentration appears to have a more significant impact than having calcium present when bound to CaCO₃.

A one-way ANOVA revealed that there were statistically significant differences between the hydrogel formulations and their respective gelling times ($p = 3.3 \times 10^{-9}$). Tukey–Kramer's test for pairwise comparisons found multiple differences between the hydrogels (Table 3). The gelation times for formulation 10-L (C/G 0.4/0.4) was significantly different from all formulations. Noticeable differences and trends between the low, medium and high concentration hydrogels were observed. Additionally, gelling time was found to be tunable, decreasing with higher concentrations of both GDL and CaCO₃. Additionally, all hydrogels exhibited a storage modulus significantly greater than their loss moduli and had a G^* of at least 35 Pa at 1 Hz.

The observed influence of the hydrogel composition on G^* is detailed in Figure 3. When the Ca²⁺:alginate and GDL:CaCO₃ ratios were 0.500–1.000 mol:mol and 0.125–0.250 mol:mol, respectively, G^* gradually increased with time and respective gelation times were among the lowest (formulations 10, 11, 12, 13, 14, 15, 18), ranging from 1517 to 2803 s, or 20 to 48 min. When the Ca²⁺:alginate and GDL:CaCO₃ ratios were 1.000–1.500 mol:mol and 0.250–0.500 mol:mol respectively, G^* increased more rapidly with time and respective gelation times ranged 1055–1400 s, or 17–23 min (formulations 16, 19, 20). Lastly, when Ca²⁺:alginate and GDL:CaCO₃ mol concentrations were 0.500–1.000 and 0.125–0.250 mol:mol respectively, G^* dramatically increased within a short period of time and respective gelation times were among the fastest, averaging 660–707 s or around 11 min to gel completely (formulations 17, 21). Additionally,

TABLE 3 Post-hoc comparisons using Tukey–Kramer's test

	10-L	11	12	13	14	15	16-M	17	18	19	20	21-H
10-L		780*	1600*	720*	510*	1200*	1530*	2080*	630*	1400*	1700*	2100*
11			800*	58	280	460*	750*	2000*	150	670*	970*	1300*
12				860*	1080*	350	50	500*	960*	140	170	490*
13					220	510*	810*	1400*	98	720*	1020*	1300*
14						730*	1030*	1600*	120	940*	1200*	1600*
15							300	840*	610*	210	510*	840*
16-M								550*	910*	85	220	540*
17									1500*	630*	330	8.0
18										820*	1100*	1400*
19											300	630*
20												330
21-H												

Note: The mean differences between gelation times of hydrogel formulations 10–21 were recorded. Significance at the $p < 0.05$ level is indicated by asterisk (*). Nonsignificant comparisons are bolded. Slight grouping between low (10-L), medium (16-M), and high (21-H) GDL:CaCO₃ concentration hydrogels was observed.

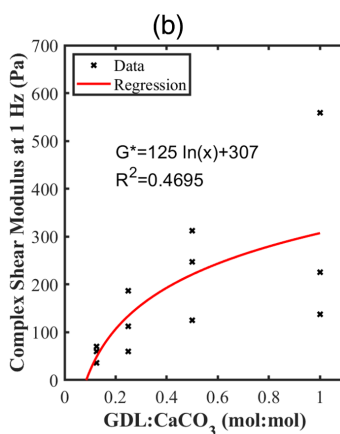
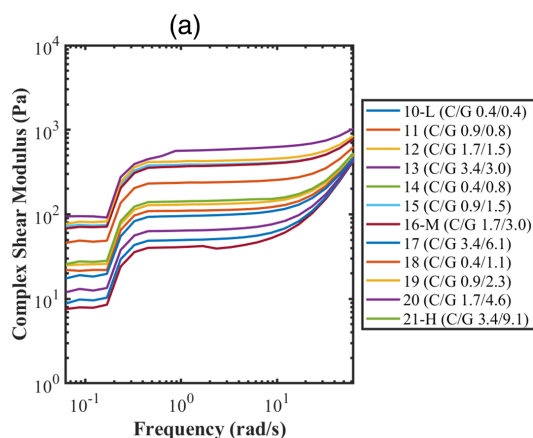


FIGURE 4 Frequency sweep results of hydrogel formulations. (a) Frequency sweep data from hydrogel formulations 10–21 performed in triplicate ($n = 3$). There is a positive exponential relationship between increasing frequency and complex shear modulus. (b) Complex shear modulus (G^*) as a function of concentration ratio (CaCO₃:GDL) from hydrogel formulations 10–21 at low frequencies. GDL:CaCO₃ ratios significantly influence G^* , with higher ratios contributing to high complex shear moduli, as determined by two-tailed t -test ($p < 0.05$).

each group was statistically different from each other ($p = 0.0447$), confirming that these ratios can significantly influence gelation times.

Immediately following the gelation test, a frequency sweep was run on each hydrogel sample in triplicate with the result reported as the average \pm SD ($n = 3$). Figure 4 details the viscoelastic properties of the alginate hydrogels. Similar to the grouping for the gelation test, there was further grouping observed between low, medium and high concentration alginate hydrogels. The lower crosslinker concentration hydrogels (GDL:CaCO₃ ratios of 0.125 and 0.250) corresponded with softer hydrogels whereas higher crosslinker concentration hydrogels (GDL:CaCO₃ ratios of 0.5 and 1.0) were stiffer. The data show that by varying the components of the gels, a significant influence on complex shear modulus and gelation time were observed ($p < 0.05$). Furthermore, there were no significant differences in complex shear modulus at 1% strain and 1 Hz with or without MB ($p = 0.550$, 0.998, and 0.560, respectively for formulations 10-L, 16-M, and 21-H) ($n = 3$).

The strain amplitude response of low, medium, and high concentration hydrogels of both CaCO₃ and GDL, GDL:CaCO₃ ratios of 0.125, 0.500 and 1.00, respectively (10-L, 16-M, 21-H), were evaluated via amplitude sweep. A one-way ANOVA was used to determine

whether storage modulus (G') differed between formulations 10, 16, and 21. Low (formulation 10) and high (formulation 21) concentration hydrogels and medium (formulation 16) and high concentration hydrogels were significantly different from each other ($p = 0.0021$ and 0.0006, respectively). The storage modulus (G') increased from low to high concentration hydrogels. All hydrogels contained a linear viscoelastic (LVE) region response to dynamic shear stress, up to at least 10% strain (Figure 5). Formulations 16-M and 21-H were damaged at higher strains. Formulation 21-H demonstrates a sharp increase in complex shear stress followed by a decrease around 20% complex shear strain, indicative of hydrogel “fracturing.”

3.3 | Swelling and MB release of alginate hydrogels

The swelling and MB release profile of the hydrogels was recorded in vitro over a period of 14 days (Figures 6B and 7A, respectively). The degree of equilibrium swelling varied among hydrogels, ranging from 0% to 150%. Formulations 12 and 21-H had the lowest and

highest swelling percentage, respectively, correlating to low and high GDL:CaCO₃ ratios, 0.125 and 1.00, respectively. The degree of swelling variations is indicative of the components within the hydrogels. Low and medium concentration (GDL:CaCO₃ ratios of 0.125 and 0.5, respectively) hydrogels had degrees of swelling reported around 100%–120%, whereas high concentration hydrogels exhibited swelling above 120%.

Low concentration hydrogels among all time points displayed the lowest degree of swelling over time whereas higher concentration hydrogels had the highest degree of swelling, as expected. CaCO₃ values were found to influence swelling over time with the lowest GDL:CaCO₃ ratio swelling most rapidly. The ratio of Ca²⁺:alginate was the primary driver of hydrogel swelling with the highest ratios swelling the most overall. For formulations 10-L, 16-M, and 21-H, swelling was significantly different for all time points after day 1, with 10-L swelling the least and 21-H swelling the most. Formulation 21-H had significantly increased swelling compared to the other formulations at all-time points. Hydrogels prepared with Ca²⁺:alginate ratio of 0.50 were at approximately equilibrium swelling as formed.

Table 4 compares swelling data for formulations 10-L, 16-M, and 21-H both with and without MB incorporated. While most of these differences were not statistically significant, it can be noted that formulations without MB swelled slightly more than formulations with MB, particularly at early time points. This was true for all formulations on days 1 and 2. By day 7, this difference was no longer seen for formulation 10-L, but was amplified in formulations 16-M and 21-H. On

days 7 and 12, the SDs increased, likely due to gels losing crosslinks over time.

MB release from the hydrogel formulations is further detailed in Figure 7. Among all hydrogels, an initial burst release was observed within the first 5 days, with over 50% MB released. Following the initial burst, a slower and more sustained release followed until the hydrogels disintegrated. Lower concentration hydrogels had the most cumulative MB release (~90%) by 12 days, the point at which the alginate hydrogels were mostly disintegrated and released remaining MB. The formulations with the fastest release rate had the lowest GDL:CaCO₃ ratios (0.125). Furthermore, formulation 14 had the fastest release rate and also had the lowest GDL concentration. The formulations (13, 17, 21-H) with the lowest values of MB release had the highest values of GDL:CaCO₃ (1.000). The solubility limit of MB in water is 43.6 mg/ml which is several orders of magnitude higher than the amount that was released from the gels. However, it is possible that diffusion may have been limited by the concentration of MB in the eluent at later time points due to the long period between sampling.

3.4 | Hydrogel degradation

Naturally derived biomaterials can be advantageous for drug delivery applications as their components can be broken down and/or eliminated by the body. Degradation of alginate can be more challenging

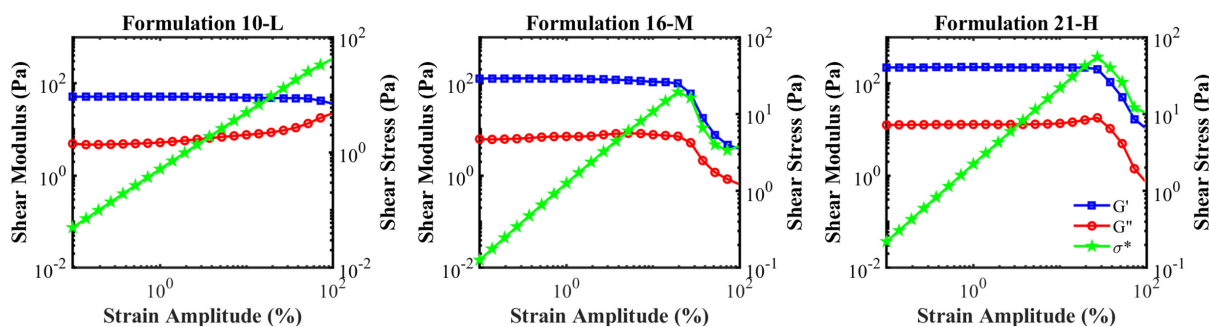


FIGURE 5 Rheological characterization of hydrogel formulations. Amplitude sweep data from representative hydrogels ($n = 3$). Formulations 10-L, 16-M, and 21-H represent low, medium and high GDL:CaCO₃ concentrations with ratios of 0.125, 0.500 and 1.00, respectively. A linear viscoelastic region of stiffness response corresponding to 1 Hz dynamic shear is observed up to 1% strain, with formulation 10-L exhibiting LVE past 20%.

TABLE 4 Differences in swelling for hydrogels with (+) and without (–) MB

Formulation ID	Formulation name	Day 1 swelling (%)	Day 2 swelling (%)	Day 7 swelling (%)	Day 12 swelling (%)
10-L MB-	C/G 0.4/0.4	116 ± 4	105 ± 4	91 ± 7	98 ± 13
10-L MB+	C/G 0.4/0.4 with MB	112 ± 9	93 ± 10	100 ± 8	106 ± 14
16-M MB-	C/G 1.7/3.0	108 ± 10	104 ± 13	181 ± 37	100 ± 27
16-M MB+	C/G 1.7/3.0 with MB	104 ± 7	102 ± 15	146 ± 23	130 ± 9
21-H MB-	C/G 3.4/9.1	129 ± 9	121 ± 17	234 ± 61	226 ± 24
21-H MB+	C/G 3.4/9.1 with MB	113 ± 4	107 ± 2	165 ± 6	190 ± 9

Note: Swelling was higher for formulations without MB at early time points ($n = 5$).

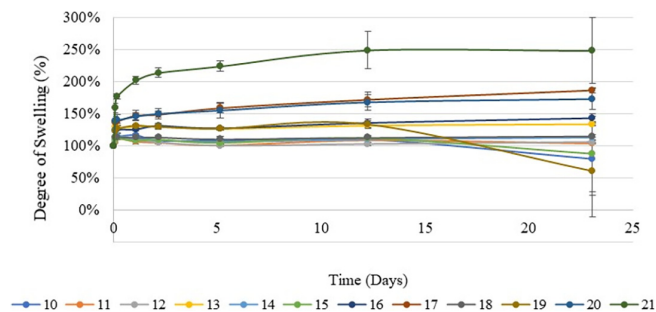


FIGURE 6 Swelling data of hydrogel formulations over 25 days. After 12 days, the integrity of the hydrogels became compromised. Degree of swelling ranged from 100% to 250%, with CaCO_3 content significantly influencing the degree ($p = 0.0317$) ($n = 3$). For formulations 10-L, 16-M, and 21-H, swelling was significantly different for all time points after day 1, with 10-L swelling the least and 21-H swelling the most. Formulation 21-H had significantly increased swelling compared to the other formulations at all-time points.

than other biomaterials as the hydrogel breaks down by ion exchange, decrosslinking the polymers. The *in vitro* degradation of alginate hydrogels was studied for 2 weeks with the initial and final masses recorded (mg). Table 5 summarizes the degradation results of hydrogel formulations 10–21.

To better characterize the degradation of the hydrogels, samples were taken at days 0, 1, 3, 7, and 14. The mass change of the hydrogels significantly increased following immersion in 1X DPBS from 8.0 ± 1.2 to 18 ± 5.4 mg ($p < 0.05$). A two-way ANOVA with Tukey post-hoc analysis found significant differences between the days ($p < 0.0001$) but not between each formulation ($p > 0.561$).

Swelling rates (and subsequent mass change) varied significantly on days 0 and 14 based on hydrogel composition. Higher concentration hydrogels displayed the highest degree of swelling on day 0; however, on day 14, low concentration hydrogels displayed the highest degree of swelling. The average mass of the hydrogels (mg) following 0, 1, 3, 7, and 14 days were 8.0 ± 1.2 , 12.7 ± 1.0 , 12.0 ± 0.76 , 12.3 ± 2.4 , and 18.3 ± 5.4 , respectively.

For days 1, 3, and 7 of incubation, the degree of swelling as well as the average mass did not significantly differ from each other ($p > 0.970$). Day 0 and day 14 differed significantly from all timepoints ($p < 0.006$), with greater statistical difference between the two ($p < 0.00001$). There were observable groups between the low, medium and high concentration hydrogels (10-L, 16-M, 21-H), with the low and higher concentration gels displaying higher degrees of swelling and percentage mass change. There were no significant differences seen between hydrogels 10-L, 16-M, and 21-H when compared with and without the addition of MB.

3.5 | Cytotoxicity of alginate hydrogels

A fundamental requirement for any drug delivery system is minimal cytotoxicity. To this end, following the synthesis of our

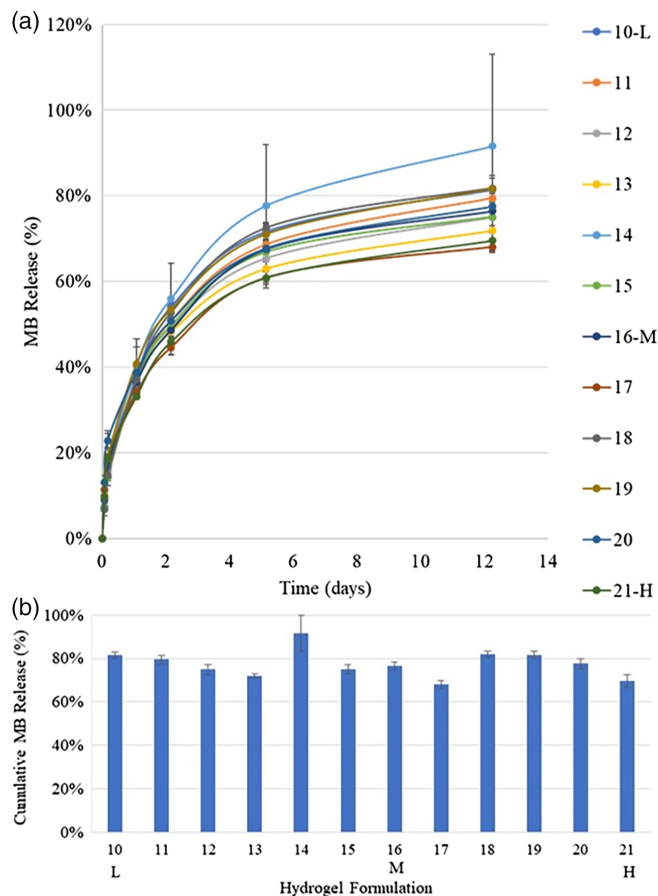


FIGURE 7 Methylene blue release. (a) The release profile of methylene blue (MB) from hydrogel formulations 10–21 ($n = 3$). The formulation with the fastest release rate (14) had the lowest GDL: CaCO_3 ratio (0.125) and lowest GDL concentration. The formulations with the lowest values of MB release had the highest values of GDL: CaCO_3 (1.000). (b) The cumulative release of MB from hydrogels recorded at day 12 ($n = 3$). The hydrogels composed of 0.5 GDL: CaCO_3 molar ratios (medium concentration) had the highest release profile of low and high concentration hydrogels at each time point.

representative hydrogels, we studied their biocompatibility using human retinal pigment epithelial cells. ARPE-19 cells were incubated with the representative hydrogels for 48 h and assessed via MTS assay. As shown in Figure 8, all formulations demonstrated excellent biocompatibility with ARPE-19 cells during the 48 hour incubation. We found that cellular viability normalized to base media control for all hydrogels, ranged from 93% to 95%. A one-way ANOVA with a Tukey–Kramer's post-hoc test additionally found that there was no statistically significant difference between each hydrogel formulation ($p > 0.630$). Additionally, there was no statistically significant difference between the hydrogel formulations and the media control ($p > 0.348$). Alginate hydrogels have proven to be biocompatible in various studies^{15,16} and our results further support its minimal toxicity to retinal cells and suggest the potential of the injectable alginate hydrogels for future evaluation in *in vivo* ophthalmic models.

TABLE 5 Hydrogel degradation results

Formulation	Day 0 (mg)	Day 1 (mg)	Day 3 (mg)	Day 7 (mg)	Day 14 (mg)
10-L	6.4 ± 0.5	12.2 ± 0.2	11.5 ± 0.8	10.3 ± 1.4	24.9 ± 2.2
11	6.4 ± 0.5	13.5 ± 1.0	12.2 ± 0.3	10.5 ± 0.7	24.9 ± 11.0
12	8.0 ± 0.5	12.8 ± 0.5	11.7 ± 0.3	10.6 ± 0.9	13.7 ± 1.4
13	9.6 ± 0.2	14. ± 2.9	12.2 ± 0.8	12.0 ± 0.8	21.3 ± 6.0
14	6.7 ± 0.6	13.8 ± 1.8	13.2 ± 0.3	11.1 ± 0.4	27.7 ± 10.7
15	7.7 ± 0.2	12.6 ± 2.3	11.4 ± 1.1	10.5 ± 0.4	11.8 ± 0.6
16-M	8.5 ± 0.2	12.3 ± 1.3	11.0 ± 0.1	11.4 ± 0.7	13.8 ± 2.7
17	9.9 ± 0.3	11.4 ± 0.6	11.8 ± 3.2	11.4 ± 0.7	16.1 ± 1.9
18	7.2 ± 0.5	13.7 ± 0.5	12.3 ± 1.1	12.9 ± 7.5	14.7 ± 5.4
19	7.8 ± 0.3	12.8 ± 0.5	11.1 ± 0.9	17.6 ± 3.0	14.0 ± 1.3
20	8.5 ± 0.5	12.9 ± 2.0	12.4 ± 2.6	13.4 ± 1.1	15.5 ± 3.6
21-H	9.3 ± 0.8	10.6 ± 0.9	13.4 ± 3.4	16.3 ± 0.9	20.9 ± 8.8

Note: The masses of hydrogel formulations 10–21 were recorded over 14 days following immersion in 10 ml 1X DPBS and weighed at 0, 1, 3, 7, and 14-day timepoints following lyophilization.

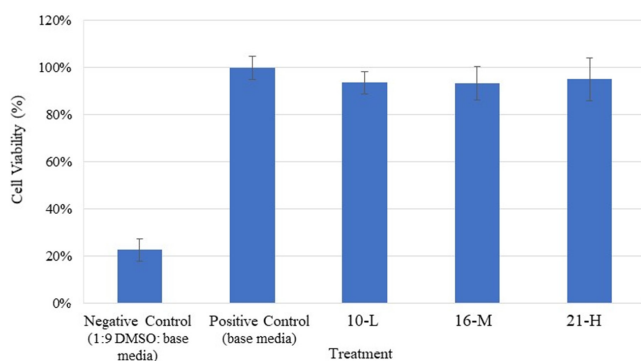


FIGURE 8 Cytotoxicity of representative hydrogels. Cell viability as measured by optical density (OD) of the MTS reagent product following exposure to alginate hydrogels. The low, medium, and high concentration hydrogels that were evaluated maintained a cell viability of at least 93% of that of the positive control base media (DMEM/F12, 10% FBS, 1% PS). No significant differences were noted between the low, medium, and high concentration hydrogels (10-L, 16-M, 21-H) ($n = 3$).

3.6 | MB as a ROS scavenger

Scavenging of ROS by MB was evaluated through in vitro testing based on published methods.²⁵ We hypothesized that because MB is a proven ROS scavenger, MB loaded into these hydrogels would effectively scavenge ROS. ARPE-19 cells were first incubated with MB concentrations of 0.0, 0.05, 0.25, 0.50, 1.0, and 2.0 mg/ml for 24 h and then treated with H₂O₂ for 24 h. ROS levels/activity was characterized by the appearance of highly fluorescent compound DCF in the DCFH-DA assay. There was an observable decrease in fluorescence in cell culture corresponding to increased MB concentration. We confirmed that ROS levels decreased significantly with MB concentrations of 0.50, 1.0 and 2.0 mg/ml ($p < 0.05$) (Figure 9). These results suggest the potential of using MB as a ROS scavenger for ocular applications, particularly for neural cells.

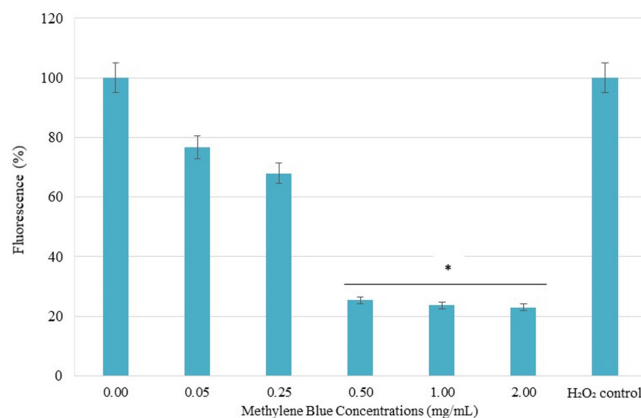


FIGURE 9 Methylene blue ROS results. ROS activity measured by DCF fluorescence in ARPE-19 cells induced by 600 μ M H₂O₂. Increased concentrations of methylene blue contributed to higher cell survival during prolonged exposure to H₂O₂. Data ($n = 5$) is presented as mean \pm SD. Results were normalized against H₂O₂ control. Higher fluorescence is indicative of greater DCF presence, more ROS activity and lowered cell survivability. Differences in the fluorescence of MB concentrations of 0.5, 1.0, and 2.0 mg/ml were found to be statistically significant ($p < 0.05$).

The ability to scavenge ROS was confirmed with MB. Additional studies were performed with alginate to further confirm MB's ROS scavenging ability while loaded into a hydrogel (Figure 10). All hydrogels were loaded with 1.0 mg/ml MB, except the negative control, formulation 16-M, which was additionally tested without MB. ARPE-19 cells were incubated with hydrogel formulations 10-L, 16-M, 16-M without MB, and 21-H for 24 h. Following incubation, the hydrogels and cells were exposed to H₂O₂ for 24 h with resulting DCF fluorescence measured. All alginate hydrogels demonstrated ARPE-19 survival of >40% when exposed to the oxidative stressor H₂O₂. Differences between the formulations were not statistically significant ($p > 0.05$). The presence of MB was found to significantly influence

cell survival when loaded into medium hydrogel formulation 16-M ($p < 0.05$), decreasing from 43% with MB to ~30% without.

3.7 | Injection feasibility

In addition to demonstrating sustained therapeutic release, ROS scavenging ability, and acceptable in vitro biocompatibility, these hydrogel scaffolds are also injectable. To demonstrate this ability, injection tests were conducted in triplicate using 22, 25, and 30-gauge needles as shown in Figure 11. Hydrogels were injected as both a liquid and gel onto a microscope slide to verify injectability. Videos demonstrating injection feasibility are available in Supporting Information S1. In these videos, MB was also added to the gels and shown to not influence injection feasibility through 22 or 27-gauge needles. Gels formed after being dispensed onto the glass plates. In clinical application for TON treatment, the alginate hydrogel would be injected as a liquid and form a gel in situ in the retrobulbar space behind the eye. We also validated the ability to inject a pre-formed alginate hydrogel through

the needle in the event the gel forms prior to injection, even though we have specifically tuned gelation times to prevent this potential complication. Alginate hydrogels were easily injected as liquid prior to gel formation through every needle gauge tested. The pre-formed alginate hydrogel could not be injected through a 30-gauge needle, but could be easily injected through larger diameter needles, including the 25-gauge needle, which is commonly used for ocular drug delivery.

4 | DISCUSSION

In this study, we developed an injectable drug-loaded vehicle for local delivery of MB around the optic nerve following injury to address the shortage of treatment options for TON. Sustained MB release was achieved among all synthesized alginate hydrogel formulations and may be suitable for treating optic neuropathy as well as other ocular injuries.

As reported in Table 1, alginate hydrogels were synthesized by internal crosslinking with evenly distributed insoluble calcium carbonate (CaCO_3) and a slow hydrolyzing proton donor, GDL. This method slows down the rate of gelation to ~10–50 min, accommodating adequate mixing of all components and subsequent injection through a small gauge needle.

Hydrogel formulations 1–9 were prepared based on their ability to consistently form solid hydrogels. Molar ratios of $\text{GDL}:\text{CaCO}_3$ were found to influence pH values of the hydrogels, with concentrations greater than 2.0 contributing to a decrease in pH values. Formulations 10–21 were then prepared after design of experiments and evaluated based on preliminary data from Formulations 1–9, as well as demonstrating physiological pH values of 6–8.

Alginate hydrogels are formed by ionic crosslinking. Calcium ions form these ionic crosslinks with alginate polymers by attracting the carboxyl group from two adjacent alginate monomers between two polymer chains. Hypothetically, maximum crosslinking would occur when four moles of alginate monomer are present for every one mole of Ca^{2+} . However, calcium will crosslink only the guluronic acid monomers. This particular alginate has slightly more mannuronic acid than guluronic acid (~60/40), which could slightly offset the values from the hypothetical maximum. All CaCO_3 concentrations of

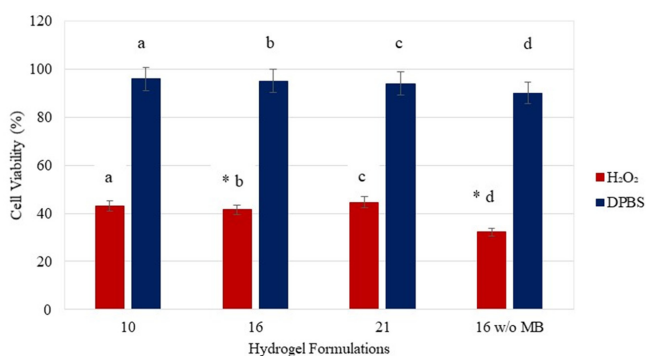


FIGURE 10 Hydrogel ROS scavenging. As expected, the number of viable cells significantly decreased for each formulation following exposure to H_2O_2 (as denoted by lower case letters a, b, c, d). Cell viability, as referenced to untreated control, was maintained at over 40% for formulations with MB incorporated in the hydrogels. Differences between formulation 16 with and without MB was found to be statistically significant ($*p < 0.01$), demonstrating MB incorporation had a significant effect on cell viability after exposure to oxidative stress ($n = 3$).

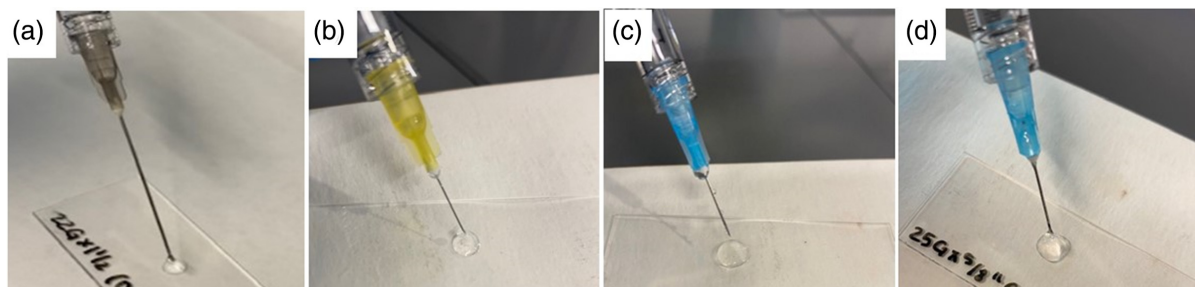


FIGURE 11 Injection feasibility. Injection of liquid hydrogel formulation through a (a) 22-gauge and (b) 30-gauge needle. Injection feasibility of a representative alginate hydrogel as (c) liquid and (d) pre-formed gel through a 25-gauge needle ($n = 3$).

hydrogel formulations in this study were prepared based on Ca^{2+} :alginate molar ratios approximately equal to and slightly greater than and less than this crosslinking maximum.

Hydrogel formulations were evaluated by rheological testing. Results confirmed the gel-like nature of the alginate hydrogels ($G' > G''$) and all formed gels within 1 h. Viscoelasticity was influenced by the ratios of GDL: CaCO_3 and the weight percent of alginate. Hydrogels with low concentrations of GDL and CaCO_3 had G' values of around 20 Pa, medium gels ~ 35 Pa and high concentration gels of ~ 95 Pa ($p < 0.05$). Hydrogels were targeted to mimic the mechanical properties of soft nerve tissues. As expected, a higher Ca^{2+} concentration induced stronger gelation which is evident in our results.^{27,30} Future studies may focus on increasing Ca^{2+} concentrations to higher concentration levels to increase modulus for other applications. Additionally, higher concentration hydrogels gelled significantly faster than low and medium hydrogels ($p < 0.05$), with formulations 10-L (C/G 0.4/0.4) and 21-H (C/G 3.4/9.1) having the slowest and most rapid gelation times, respectively. Addition of MB did not have a significant effect on hydrogel mechanical properties.

GDL and CaCO_3 were primarily used to modulate hydrogel mechanical properties including viscoelasticity and stiffness in an attempt to promote a wound healing environment around the optic nerve with similar mechanical properties, due to the known influence of mechanical properties of central nervous system repair.³¹ Furthermore, we evaluated this crosslinking mechanism to tune gelation times since traditional crosslinking with free calcium ions from calcium chloride would yield a too rapid gelation for injection into the retrobulbar space, the area located behind the globe of the eye. This is the most likely route of clinical injection for optic neuropathy. However, if these gels were adapted for intravitreal injection, small volumes are capable of being injected clinically without long-term effects to intraocular pressure (e.g., 25–100 μl).³² That being said, increased pressure behind the eye, including intracranial pressure, can lead to damage to the nerve fiber layer, which has also been seen in swelling after injury.³³ Therefore, the effects of hydrogel injection on intraocular pressure, nerve fiber layer health, and optic nerve head health should be evaluated in future studies.

In this study, a positively charged therapeutic MB was delivered from a negatively charged alginate hydrogel. It is expected that the cationic MB has the ability to electrostatically interact with the anionic alginate polymer backbone. These electrostatic interactions have been employed to slow release in other systems, including alginate,³⁴ which may prove beneficial in this case where we are trying to extend release of a hydrophilic therapeutic. Release medium can also have a significant impact on the rate of therapeutic release. A study by Deepika et al.³⁵ investigated the impacts of divalent ions including Mg^{2+} and Ca^{2+} on release of anionic levofloxacin from a chitosan-alginate hybrid gel nanoparticles. Metal ions were shown to have a significant influence on nanoparticle morphology, drug encapsulation efficiency, and release profile from these nanoparticles. In this study, the presence of divalent cations impacts alginate gel structure and swelling in addition to positive charges similar to the therapeutic evaluated. The true in vivo situation for the environment of the optic nerve is of course more complex due to the presence of both physiological saline (mimicked in this study by

DPBS) and orbital fat and connective tissues. The presence of fatty tissue will likely have an effect on release of MB, slowing it compared to release directly into saline. DPBS, the only in vitro release model published for extended release in TON,¹⁴ represents a worst-case scenario for extended release for TON since it assumes all drug will be more rapidly transported out of the retrobulbar space in the aqueous phase.

Furthermore, the local dosing of MB required remains unknown. Previous studies have used an oral delivery route for MB, typically 1–4 mg/kg³⁶ to achieve a local concentration of ~ 0.5 μM in the target neural tissue.³⁷ The total MB dose required to achieve this therapeutic dose over time remains to be determined in vivo and will depend significantly on the presence and extent of injury. Loading values included in the present study were used to bracket the range of values which may be required to achieve this therapeutic concentration locally.

We used two-tailed t-tests to investigate the impact of crosslinking density in these hydrogels on MB release rates, and saw no significant difference. This is likely due to the low molecular weight (319 g/mol) and hydrophilicity of the therapeutic which would not have diffusion significantly inhibited through a lightly crosslinked alginate network. We hypothesized that short-term release of ROS scavengers such as MB would mitigate injury mechanisms, but micro- or nano-encapsulation of the therapeutic would be needed to extend therapeutic efficacy if needed.¹⁴

ARPE-19 cells were used to represent the microenvironment of the optic nerve because although primary ON cells would be preferred, their usage is limited due to difficulty in obtaining and isolating these cells and slow proliferation rates.²⁸ As such, the immortalized cell line ARPE-19 was chosen in our study. Cytotoxicity results indicated that the hydrogels demonstrated low to minimal toxicity with no statistically significant differences between low, medium and high GDL: CaCO_3 concentration hydrogels. The hydrogels maintained cell viability of over 90%. Results are consistent with previous reports of the use of alginate hydrogels and MB for drug delivery and tissue engineering applications.^{8–12,15,16}

The scavenging ability of MB was validated through both varying concentrations of MB and evaluating low, medium and high concentration hydrogels. ROS scavenging results from DCF assays indicate that MB concentrations of 0.5, 1.0, and 2.0 reduced ROS activity. Additionally the presence of MB was shown to significantly improve cell survival in the presence of oxidative stressor H_2O_2 when compared to blank alginate hydrogels. In addition to its therapeutic activity, MB did have some influence hydrogel swelling, particularly at early time points, which may be considered when using cationic therapeutics in this system.

5 | CONCLUSION

In conclusion, to improve upon the current management options for oxidative injury, particularly TON, tunable internally crosslinked sodium alginate hydrogels were developed. We also identified hydrogels with optimal mechanical properties and drug release by modulating components using design of experiments. The designed alginate drug delivery

system is biocompatible and adequately lowers the concentration of ROS in vitro. Most importantly, the proposed design improves upon the current treatments for TON: by offering local delivery of ROS scavengers, deleterious off-target effects of such drugs can be avoided. Modifying the ratios of CaCO₃ to GDL impacted hydrogel swelling, mechanical properties, and release of cationic therapeutic MB. Given the results of the drug release as well as its biocompatibility and injectability, alginate hydrogels with higher concentrations of CaCO₃ and GDL have the potential to improve TON damage as well as other diseases in which there is an accumulation of reactive species, which will be validated in vivo in future studies.

AUTHOR CONTRIBUTIONS

Courtney J. Maxwell, Andrew M. Soltisz, Matthew A. Reilly, and Katelyn E. Swindle-Reilly planned the experiments. Courtney J. Maxwell, Andrew M. Soltisz, Wade W. Rich, and Andrew Choi carried out the experiments. Courtney J. Maxwell, Andrew M. Soltisz, Wade W. Rich, Matthew A. Reilly, and Katelyn E. Swindle-Reilly contributed to the interpretation of the results. Courtney J. Maxwell, Andrew M. Soltisz, Matthew A. Reilly, and Katelyn E. Swindle-Reilly drafted the manuscript. Matthew A. Reilly and Katelyn E. Swindle-Reilly conceived the study and were in charge of overall direction and planning.

ACKNOWLEDGMENTS

The authors would like to acknowledge undergraduate students Emma McLaughlin, Marissa Ruzga, and Samantha Thobe, who contributed to preliminary studies and data visualization. Graduate student Megan Allyn assisted with cell culture. Additionally, we would also like to thank Dr. Aleksander Skardal for providing the fluorescent plate readers and Dr. Colleen Cebulla for providing retinal cells.

FUNDING INFORMATION

Supported by the US Department of Defense Vision Research Program Award W81XWH-15-1-0074. The opinions or assertions contained herein are the private views of the authors and are not to be construed as official or as reflecting the views of the Department of the Army or the Department of Defense.

CONFLICT OF INTEREST

The authors declare no conflict of interest.

DATA AVAILABILITY STATEMENT

The data generated during and/or analyzed during this study are available on request from the corresponding author.

ORCID

Matthew A. Reilly  <https://orcid.org/0000-0001-8029-0084>

Katelyn E. Swindle-Reilly  <https://orcid.org/0000-0003-1739-0263>

REFERENCES

- Steinsapir KD, Goldberg RA. Traumatic optic neuropathy. *Surv Ophthalmol.* 1994;38:487-518.

- Pirouzmand F. Epidemiological trends of traumatic optic nerve injuries in the largest Canadian adult trauma center. *J Craniofac Surg.* 2012; 23:516-520.
- Weichel ED, Colyer MH, Bautista C, Bower KS, French LM. Traumatic brain injury associated with combat ocular trauma. *J Head Trauma Rehabil.* 2009;24:41-50.
- Levin LA, Beck RW, Joseph MP, Seiff S, Kraker R. The treatment of traumatic optic neuropathy: the international optic nerve trauma study. *Ophthalmology.* 1999;106:1268-1277.
- Wells J, Kilburn MR, Shaw JA, et al. Early in vivo changes in calcium ions, oxidative stress markers, and ion channel immunoreactivity following partial injury to the optic nerve. *J Neurosci Res.* 2012;90: 606-618.
- O'Hare Doig RL et al. Reactive species and oxidative stress in optic nerve vulnerable to secondary degeneration. *Exp Neurol.* 2014;261: 136-146.
- Xiong ZM, Choi JY, Wang K, et al. Methylene blue alleviates nuclear and mitochondrial abnormalities in progeria. *Aging Cell.* 2016;15: 279-290.
- Ryou MG, Choudhury GR, Li W, et al. Methylene blue-induced neuronal protective mechanism against hypoxia-reoxygenation stress. *Neuroscience.* 2015;301:193-203.
- Duan Y, Haugabook SJ, Sahley CL, Muller KJ. Methylene blue blocks cGMP production and disrupts directed migration of microglia to nerve lesions in the leech CNS. *J Neurobiol.* 2003;57:183-192.
- Wiklund L et al. Neuro- and cardioprotective effects of blockade of nitric oxide action by Administration of Methylene Blue. *Ann N Y Acad Sci.* 2007;1122:231-244.
- Xu H, Li J, Wang Z, et al. Methylene blue attenuates neuroinflammation after subarachnoid hemorrhage in rats through the Akt/GSK-3 β /MEF2D signaling pathway. *Brain Behav Immun.* 2017;65: 125-139.
- Shen Q, du F, Huang S, Rodriguez P, Watts LT, Duong TQ. Neuroprotective efficacy of methylene blue in ischemic stroke: an MRI study. *PLoS One.* 2013;8:1-6.
- Talley Watts L, Long JA, Chemello J, et al. Methylene blue is neuroprotective against mild traumatic brain injury. *J Neurotrauma.* 2014; 31:1063-1071.
- DeJulis CR et al. Microsphere antioxidant and sustained erythropoietin-R76E release functions cooperate to reduce traumatic optic neuropathy. *J Control Release.* 2021;329:762-773.
- Tønnesen HH, Karlsen J. Alginate in drug delivery systems. *Drug Dev Ind Pharm.* 2002;28:621-630.
- Sun J, Tan H. Alginate-based biomaterials for regenerative medicine applications. *Materials (Basel).* 2013;6:1285-1309.
- Draget KI, Ostgaard K, Smidsrod O. Alginate-based solid media for plant tissue culture. *Appl Microbiol Biotechnol.* 1989;31:79-83.
- Kuo CK, Ma PX. Maintaining dimensions and mechanical properties of ionically crosslinked alginate hydrogel scaffolds in vitro. *J Biomed Mater Res A.* 2008;84:899-907.
- Kuo CK, Ma PX. Ionically crosslinked alginate hydrogels as scaffolds for tissue engineering: part 1. Structure, gelation rate and mechanical properties. *Biomaterials.* 2001;22:511-521.
- Draget KI, Østgaard K, Smidsrød O. Homogeneous Alginate gels: a technical approach. *Carbohydr Polym.* 1990;14:159-178.
- Rahmani V, Elshereef R, Sheardown H. Property modelling of lysozyme-crosslinker-alginate complexes using latent variable methods. *J Biomed Mater Res A.* 2021;109:2225-2236.
- Zuidema JM, Rivet CJ, Gilbert RJ, Morrison FA. A protocol for rheological characterization of hydrogels for tissue engineering strategies. *J Biomed Mater Res B Appl Biomater.* 2014;102:1063-1073.
- Park H, Guo X, Temenoff JS, et al. Effect of swelling ratio of injectable hydrogel compositions on chondrogenic differentiation of encapsulated rabbit marrow mesenchymal stem cells in vitro. *Biomacromolecules.* 2009;10:541-546.

24. Niu H, Li X, Li H, Fan Z, Ma J, Guan J. Thermosensitive, fast gelling, photoluminescent, highly flexible, and degradable hydrogels for stem cell delivery. *Acta Biomater.* 2019;83:96-108.
25. Stoppel WL, White JC, Horava SD, Henry AC, Roberts SC, Bhatia SR. Terminal sterilization of alginate hydrogels: efficacy and impact on mechanical properties. *J Biomed Mater Res B Appl Biomater.* 2013; 102:877-884. doi:10.1002/jbm.b.33070
26. Da Violante G et al. Evaluation of the cytotoxicity effect of dimethyl sulfoxide (DMSO) on CaCO₂/TC7 colon tumor cell cultures. *Biol Pharmaceut Bull.* 2002;25:1600-1603.
27. Voloboueva LA, Liu J, Suh JH, Ames BN, Miller SS. (R)- α -lipoic acid protects retinal pigment epithelial cells from oxidative damage. *Investig Ophthalmol Vis Sci.* 2005;46:4302-4310.
28. Lee SS et al. Biodegradable implants for sustained drug release on the eye. *Pharm Res.* 2010;27:2043-2053.
29. Varela-Fernández R, Díaz-Tomé V, Luaces-Rodríguez A, et al. Drug delivery to the posterior segment of the eye: biopharmaceutic and pharmacokinetic considerations. *Pharmaceutics.* 2020;12:269-308.
30. Lee KY, Alginate DJM. Properties and biomedical applications. *Prog Polym Sci.* 2012;37:106-126.
31. Pogoda K, Janmey PA. Glial tissue mechanics and mechanosensing by glial cells. *Front Cell Neurosci.* 2018;12:25.
32. Kotliar K, Maier M, Bauer S, Feucht N, Lohmann C, Lanzl I. Effect of intravitreal injections and volume changes on intraocular pressure: clinical results and biomechanical model. *Acta Ophthalmol Scand.* 2007;85(7):777-781.
33. Malhotra K, Padungkiatsagul T, Moss HE. Optical coherence tomography use in idiopathic intracranial hypertension. *Ann Eye Sci.* 2020;5:7.
34. Hariyadi DM, Islam N. Current status of Alginate in drug delivery. *Adv Pharmacol Pharmaceut Sci.* 2020;8886095:1-16.
35. Deepika R, Girigoswami K, Murugesan R, Girigoswami A. Influence of divalent cation on morphology and drug delivery efficiency of mixed polymer nanoparticles. *Curr Drug Deliv.* 2018;15:652-657.
36. Rodríguez P, Singh AP, Malloy KE, et al. Methylene blue modulates functional connectivity in the human brain. *Brain Imaging Behav.* 2017;11:640-648.
37. Bruchey AK, Gonzalez-Lima F. Behavioral, physiological and biochemical Hormetic responses to the Autoxidizable dye methylene blue. *Am J Pharmacol Toxicol.* 2008;3:72-79.
38. Gomathi T, Susi S, Abirami D, Sudha PN. Size optimization and thermal studies on calcium alginate nanoparticles. *IOSR Journal of Pharmacy.* 2017;1:1-7.
39. Braccini I, Pérez S. Molecular basis of Ca²⁺-induced gelation in alginates and Pectins: the egg-box model revisited. *Biomacromolecules.* 2001;2:1089-1096.

SUPPORTING INFORMATION

Additional supporting information may be found in the online version of the article at the publisher's website.

How to cite this article: Maxwell CJ, Soltisz AM, Rich WW, Choi A, Reilly MA, Swindle-Reilly KE. Tunable alginate hydrogels as injectable drug delivery vehicles for optic neuropathy. *J Biomed Mater Res.* 2022;110(10):1621-1635. doi:10.1002/jbm.a.37412